# Hyper-VIB: A Hypernetwork-Enhanced Information Bottleneck Approach for Task-Oriented Communications

Jingchen Peng\*, Chaowen Deng\*, Yili Deng\*, Boxiang Ren\* and Lu Yang<sup>†‡</sup>
\*Department of Mathematical Sciences, Tsinghua University, Beijing, China
<sup>†</sup>Wireless Technology Lab, Central Research Institute, 2012 Labs, Huawei Tech. Co. Ltd., China
Email: yanglu87@huawei.com

Abstract—This paper presents Hyper-VIB, a hypernetworkenhanced information bottleneck (IB) approach designed to enable efficient task-oriented communications in 6G collaborative intelligent systems. Leveraging IB theory, our approach enables an optimal end-to-end joint training of device and network models, in terms of the maximal task execution accuracy as well as the minimal communication overhead, through optimizing the trade-off hyperparameter. To address computational intractability in high-dimensional IB optimization, a tractable variational upper-bound approximation is derived. Unlike conventional grid or random search methods that require multiple training rounds with substantial computational costs, Hyper-VIB introduces a hypernetwork that generates approximately optimal DNN parameters for different values of the hyperparameter within a single training phase. Theoretical analysis in the linear case validates the hypernetwork design. Experimental results demonstrate our Hyper-VIB's superior accuracy and training efficiency over conventional VIB approaches in both classification and regression tasks.

Index Terms—Task-oriented communications, hyperparameter optimization, hypernetwork, information bottleneck, variational inference

#### I. Introduction

The accelerated evolution of AI has propelled its adoption across critical domains, including autonomous systems, immersive technologies (e.g. AR/VR), and holographic communication etc. These widespread integrations, identified by the International Telecommunication Union (ITU) as core deployment scenarios for emerging 6G wireless systems [1], have triggered unprecedented growth in data transmission requirements, fundamentally reshaping traditional communication paradigms. Consequently, conventional data-oriented communication frameworks [2], historically focused on complete data reconstruction and intrinsic signal properties, are giving way to task-oriented methodologies [3]-[5]. These emerging approaches focus on optimizing transmission for specific objectives like real-time inference and distributed intelligence, emphasizing efficiency and relevance over exhaustive data delivery.

Despite significant advancements, the absence of a comprehensive theoretical framework for analyzing trade-offs between communication costs and inference performance

The first two authors contributed equally to this work and ‡ marked the corresponding author.

remains a key obstacle in distributed AI. Information bottleneck (IB) theory [6] provides a promising foundation for quantifying information loss and transmission efficiency. Recent studies [3], [5] have applied IB to communication system design, aiming to balance overhead with task accuracy. Extensions such as distributed IB (DIB) theory [7], [8] adapt IB to multi-device scenarios [9]. However, these approaches often overlook channel noise and, critically, fail to enable collaborative training between device and network sides.

While recent work [10] has addressed both channel noise and collaborative training concerns, training collaborative intelligent systems requires determining hyperparameters that balance performance and cost. Although current methods, including grid search [10], random search, and Bayesian optimization [11], perform well in low-dimensional settings, they become computationally prohibitive in higher dimensions due to the independent training for each hyperparameter configuration. Hypernetworks, introduced by [12], are neural networks designed to generate weights for a target network and offer a promising alternative for hyperparameter tuning. Recent studies [13], [14] leverage hypernetworks to approximate optimal response functions [15], mapping hyperparameters directly to optimized model parameters. In communication systems, hypernetworks have also been applied to characterize the varying channel states in the encoder-decoder design [16], with higher adaptability and efficiency. However, integrating the hypernetwork into IB-based collaborative intelligent system design remains unexplored.

In this paper, we introduce Hyper-VIB, a hypernetworkenhanced framework grounded in IB theory for task-oriented communications. This approach not only enables rapid and efficient identification of optimal hyperparameters, overcoming the large computation overhead and time delay in conventional methods, but also dynamically adapts to varying channel conditions, with its effectiveness rigorously proved through theoretical analysis. Our main contributions are as follows: 1) The first scheme that combines hypernetworks with IB theory in communication systems, establishing an intelligent system for accelerated hyperparameter optimization. The system can thus adaptively select the optimal configurations based on task requirements and channel states, enabling efficient taskoriented communications; 2) Theoretical validation of the

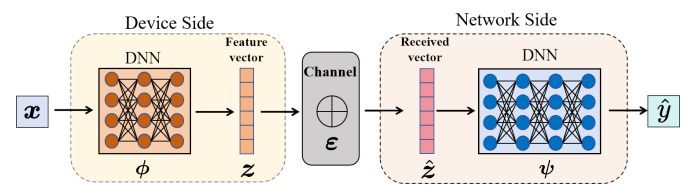


Fig. 1: The system model of device-network collaborative intelligence.

Hyper-VIB framework through optimality analysis of linear models. We establish the existence of a closed-form optimal response function that validates the hypernetwork design, providing foundational theoretical guarantees for Hyper-VIB's efficacy; 3) Development of the Hyper-IB framework with support for different kinds of intelligent tasks, including the classification tasks, and the regression tasks. Extensive experiments on image classification and wireless localization demonstrate that Hyper-VIB significantly accelerates model training while maintaining competitive performance, highlighting its broad applicability and superior performance.

# II. SYSTEM MODEL AND PROBLEM FORMULATION

This section introduces the device-network collaborative intelligence system model, illustrated in Fig. 1. In addition, our optimization problem based on the IB theory for a single link of device-network collaboration is formulated [3].

#### A. System Model and Data Transmission Chains

The input data  $\boldsymbol{x}$  at the mobile device and the target variable  $\boldsymbol{y}$  (e.g., a label) are considered as the realizations of the random variables (X,Y), characterized by the joint distribution  $p(\boldsymbol{x},\boldsymbol{y})$ . Given the dataset  $\{\boldsymbol{x}^{(m)}\}_{m=1}^{M}$ , the device and network in Fig. 1 should collaboratively infer the targets  $\{\boldsymbol{y}^{(m)}\}_{m=1}^{M}$ .

The device, upon receiving x, extracts and encodes a feature representation z. We model this combined feature extraction and encoding process as a probabilistic encoder  $p_{\phi}(z|x)$ , where  $\phi$  represents the trainable DNN parameters on the device. To establish a well-defined probabilistic model for the device, we utilize the reparameterization trick [17]. Then the conditional distribution  $p_{\phi}(z|x)$  is modeled as a multivariate independent Gaussian distribution, that is,

$$p_{\phi}(\boldsymbol{z}|\boldsymbol{x}) = \mathcal{N}(\boldsymbol{z}|\boldsymbol{\mu},\boldsymbol{\Theta}). \tag{1}$$

Here, the mean vector  $\boldsymbol{\mu} \in \mathbb{R}^d$  is determined by the DNN-based function  $\boldsymbol{\mu}(\boldsymbol{x}, \boldsymbol{\phi})$  and the covariance matrix  $\boldsymbol{\Theta}$  is structured as a diagonal matrix  $\operatorname{diag}\{\theta_1^2, \dots, \theta_d^2\}$ , where  $\boldsymbol{\theta} = (\theta_1, \dots, \theta_d)$  is produced by the DNN-based function  $\boldsymbol{\theta}(\boldsymbol{x}, \boldsymbol{\phi})$ .

Subsequently, the encoded feature z undergoes the wireless channel to the BS (i.e., network side), obtaining the received feature  $\hat{z}$ . This transmission channel, characterized by the conditional distribution  $p(\hat{z}|z)$ , is modeled as a non-trainable layer. Without loss of generality, we consider an additive white Gaussian noise channel, resulting in  $\hat{z} = z + \varepsilon$ , where  $\varepsilon \sim \mathcal{N}(\mathbf{0}, \sigma^2 \mathbf{I})$  denotes the noise with variance  $\sigma^2$ .

Finally, the network side performs inference using the received features  $\hat{z}$ . This process produces the inference

output  $\hat{y}$  via a DNN-based function  $\hat{y}(\hat{z}, \psi)$ , where  $\psi$  denotes the parameter set of the network-side DNN.

The above processes construct a Markov chain:

$$X \leftrightarrow Z \leftrightarrow \hat{Z} \leftrightarrow \hat{Y},$$
 (2)

where the random variables Z,  $\hat{Z}$  and  $\hat{Y}$  correspond to the encoded feature z, the received feature  $\hat{z}$  and the inference result  $\hat{y}$ , respectively. With this formulation, the probability equation is given by  $p(\hat{y}, \hat{z}, z|x) = p(\hat{y}|\hat{z})p(\hat{z}|z)p_{\phi}(z|x)$ .

### B. Information Bottleneck (IB) Theory

To achieve high accuracy of collaborative AI tasks with minimal wireless transmission overhead, we aim to develop the optimal AI models for both the device and network sides. According to [3], conventional IB theory provides an effective framework for the single-link collaboration. Specifically, consider the following performance metric

$$C_{\rm IB} = -I(Y; \hat{Z}) + \beta I(X; \hat{Z}), \tag{3}$$

where the objective function constitutes a weighted sum of two mutual information terms, with hyperparameter  $\beta>0$  governing the trade-off and to be discussed in detail in section III. Here, the first mutual information  $I(Y;\hat{Z})$  quantifies the information about target variable Y preserved in the networkside received features  $\hat{Z}$ , serving as a representation of inference accuracy. Meanwhile, the second term  $I(X;\hat{Z})$  evaluates the information retained in  $\hat{Z}$  conditioned on X through the minimum description length principle [18], thereby characterizing communication overhead. Consequently, a higher AI task accuracy and lower communication overhead are signified by smaller values of  $\mathcal{C}_{\text{IB}}$ , yielding the following formulation of the optimization problem

$$\min_{l} C_{IB},$$
 (4)

which is with the goal of identifying optimal AI models for device side (i.e.,  $\phi$ ) and network side (i.e.,  $\psi$ )

# C. Variational Upper Bound of $C_{IB}$

According to the definition of mutual information, calculating  $C_{IB}$  in (3) needs the conditional distribution  $p(y|\hat{z})$ for  $I(Y; \hat{Z})$  and marginal distributions  $p(\hat{z})$  for  $I(X; \hat{Z})$ . Computational challenges arise, however, from the inherent high dimensionality of input data, which impedes accurate distribution computation. We therefore leverage variational approximation [19], [20], a widely-adopted technique for approximating intractable distributions using adjustable parameters (e.g., DNN weights). Specifically, variational distribution  $r(\hat{z})$  is introduced to approximate  $p(\hat{z})$ , which is modeled as a centered isotropic Gaussian distribution  $\mathcal{N}(\hat{z}|\mathbf{0}, \mathbf{I})$  [20]. Since the inference variable  $\hat{Y}$  and the target variable Y share identical value ranges, the variational conditional distribution  $p_{\psi}(y|\hat{z})$  can be approximated by  $d(y, \hat{y}(\hat{z}, \psi))$ , where  $d(y, \hat{y})$ is the loss function to measure the distortion between y and  $\hat{y}$ , such as cross-entropy or mean squared error (MSE).

Based on the variational approximation method [19], [20], an upper bound for  $C_{IB}$  can be derived using lower and upper bounds of its mutual information terms  $I(Y; \hat{Z})$  and  $I(X; \hat{Z})$ ,

respectively. To be specific, the non-negativity property of KL divergence, i.e.  $D_{\text{KL}}(p(\boldsymbol{y}|\hat{\boldsymbol{z}})||p_{\psi}(\boldsymbol{y}|\hat{\boldsymbol{z}})) \geq 0$ , implies the existence of a lower bound for  $I(Y;\hat{Z})$  as

$$I(Y; \hat{Z}) \ge \int p(\hat{\boldsymbol{z}}, \boldsymbol{y}) \log \frac{p_{\boldsymbol{\psi}}(\boldsymbol{y}|\hat{\boldsymbol{z}})}{p(\boldsymbol{y})} d\hat{\boldsymbol{z}} d\boldsymbol{y}.$$
 (5)

Similarly, the non-negativity of  $D_{\text{KL}}(p(\hat{z})||r(\hat{z}))$  enables derivation of an upper bound for  $I(X; \hat{Z})$  given by

$$I(X; \hat{Z}) \le \int p(\hat{z}, \boldsymbol{x}) \log \frac{p_{\phi}(\hat{z}|\boldsymbol{x})}{r(\hat{z})} d\hat{z} d\boldsymbol{x}.$$
 (6)

By combining (5) and (6), we can derive an upper bound of  $C_{IB}$  ignoring a constant term of H(Y) as

$$C_{\text{VIB}}(\boldsymbol{\phi}, \boldsymbol{\psi}) = \mathbb{E}_{p(\boldsymbol{x}, \boldsymbol{y})} \Big\{ \mathbb{E}_{p_{\boldsymbol{\phi}}(\hat{\boldsymbol{z}}|\boldsymbol{x})} [-\log p_{\boldsymbol{\psi}}(\boldsymbol{y}|\hat{\boldsymbol{z}})] + \beta D_{\text{KL}}(p_{\boldsymbol{\phi}}(\hat{\boldsymbol{z}}|\boldsymbol{x}) || r(\hat{\boldsymbol{z}})) \Big\}.$$
(7)

Note that  $\hat{z} = z + \varepsilon$  with  $\varepsilon \sim \mathcal{N}(0, \sigma^2 I)$  and  $\varepsilon$  is independent of x and z, according to (1), the conditional probability density function for  $\hat{z}$  is expressed as

$$p_{\phi}(\hat{\boldsymbol{z}}|\boldsymbol{x}) = \mathcal{N}(\hat{\boldsymbol{z}}|\boldsymbol{\mu}, \boldsymbol{\Theta} + \sigma^2 \boldsymbol{I}). \tag{8}$$

Therefore, the KL divergence  $D_{\text{KL}}(p_{\phi}(\hat{z}|x)||r(\hat{z}))$  is computable through its definition as

$$D_{KL}(p_{\phi}(\hat{z}|x)||r(\hat{z})) = \frac{1}{2} \left( \|\mu\|^2 + \sum_{i=1}^{d} (\theta_i^2 + \sigma^2) - \sum_{i=1}^{d} \log(\theta_i^2 + \sigma^2) - d \right).$$
(9)

## III. THE HYPER-VIB APPROACH

The IB objective in (3) highlights the critical role of the hyperparameter  $\beta$  in achieving the optimal performance. Traditional methods, including the grid search and the random search, require retraining the model for each fixed  $\beta$ , leading to high computational cost and intolerable time delay.

To address this, we propose Hyper-VIB in this section, which enables efficient determination of optimal model parameters with diverse values of  $\beta$  within a single training run. Particularly, we formulate a best-response function that maps  $\beta$  to the optimal model parameters and explicitly model this function with a hypernetwork. Furthermore, we justify the validity of the hypernetwork architecture by demonstrating that, under a linear model, it can represent the optimal response at the device end.

# A. Hypernetwork for Best Response

We begin by constructing the best-response function [15]

$$\phi^*(\beta), \psi^*(\beta) = \arg\min_{\phi, \psi} C_{\text{VIB}}(\beta).$$
 (10)

This function maps the hyperparameter  $\beta$  to the corresponding optimal DNN parameters:  $\phi^*(\beta)$  for the device side and  $\psi^*(\beta)$  for the network side, both trained with  $\beta$ .

Next, the hypernetwork is employed to model the best-response function, which is a single neural network designed to generate parameters for a family of target networks, offering advantages such as weight sharing, dynamic tuning, and high efficiency [12], [16]. In this paper,  $\phi^*(\beta)$  and  $\psi^*(\beta)$  are regarded as the target networks. Inspired by [13], we construct

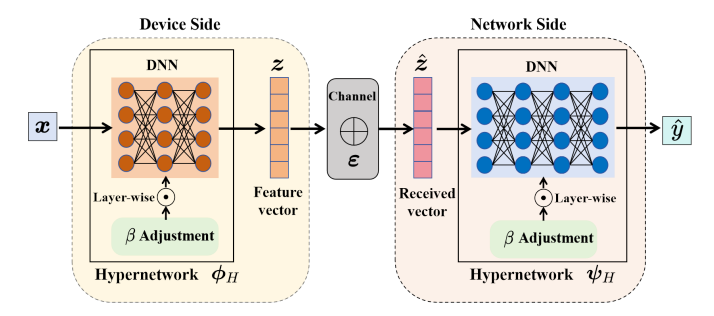


Fig. 2: The hypernetwork framework with DNN and  $\beta$  adjustment module in Hyper-VIB.

efficient hypernetworks while ensuring no significant increase in storage requirements or training time.

As shown in Fig. 2, our hypernetwork consists of two main components: the original DNN and the  $\beta$  adjustment module, which introduces the influence of the hyperparameter  $\beta$  at each network layer. Together, these components form two hypernetworks:  $\phi_H$  on the device side and  $\psi_H$  on the network side. When  $\beta$  is fixed, these hypernetworks generate the corresponding parameters,  $\phi_H(\beta)$  and  $\psi_H(\beta)$ , which approximate the best-response function in (10).

Then, we focus on how the  $\beta$  adjustment module applies layer-wise adjustments on the DNNs in our hypernetwork. Specifically, we consider both fully connected and convolutional layers, as described below.

1) Fully connected layers: Let the input feature to the *i*-th layer be  $d^{(i-1)} \in \mathbb{R}^{D_{i-1}}$ , and the output feature be  $d^{(i)} \in \mathbb{R}^{D_i}$ . Denote the weights for this layer as  $W^{(i)} \in \mathbb{R}^{D_i \times D_{i-1}}$  and the biases as  $b^{(i)} \in \mathbb{R}^{D_i}$ . The output is computed as

$$\mathbf{d}^{(i)} = \mathbf{W}^{(i)} \mathbf{d}^{(i-1)} + \mathbf{b}^{(i)}. \tag{11}$$

With the  $\beta$  adjustment module now introduced, the parameters for this layer are adjusted as follows:

$$\mathbf{W}^{(i)}(\beta) = S^{(i)} \left( \mathbf{u}^{(i)} \log(\beta) + \mathbf{v}^{(i)} \right) \odot_{\text{row}} \mathbf{W}^{(i)},$$
  
$$\mathbf{b}^{(i)}(\beta) = S^{(i)} \left( \mathbf{u}^{(i)} \log(\beta) + \mathbf{v}^{(i)} \right) \odot \mathbf{b}^{(i)}.$$
 (12)

Here,  $S^{(i)}$  is the activation function, in particular, the sigmoid function. The symbols  $\odot$  and  $\odot_{\text{row}}$  denote element-wise and row-wise multiplication, respectively. In (12),  $\boldsymbol{u}^{(i)}$ ,  $\boldsymbol{v}^{(i)} \in \mathbb{R}^{D_i}$  perform an affine transformation on  $\log(\beta)$  to obtain scaling factors, with  $S^{(i)}$  ensuring that the scaling remains within the range [0,1]. Among these,  $\boldsymbol{W}^{(i)}$  and  $\boldsymbol{b}^{(i)}$  are the original DNN parameters, while  $\boldsymbol{u}^{(i)}$  and  $\boldsymbol{v}^{(i)}$  in  $\mathbb{R}^{D_i}$  are the  $\beta$  adjustment module parameters, together forming the hypernetwork parameters at the i-th layer. This configuration shows that, compared to the original model, our hypernetwork introduces only  $2D_i$  additional parameters at this layer, demonstrating its compactness and memory efficiency. Therefore, the output  $\boldsymbol{d}^{(i)}$  can be expressed as

$$d^{(i)} = S^{(i)} \left( u^{(i)} \log(\beta) + v^{(i)} \right) \odot \left( W^{(i)} d^{(i-1)} + b^{(i)} \right).$$
 (13)

The layer-wise hypernetwork design is depicted in Fig. 3.

2) Convolutional layers: Consider the (i-1)-th layer with  $C_{i-1}$  filters, the i-th layer with  $C_i$  filters and kernel size  $K_i$ .

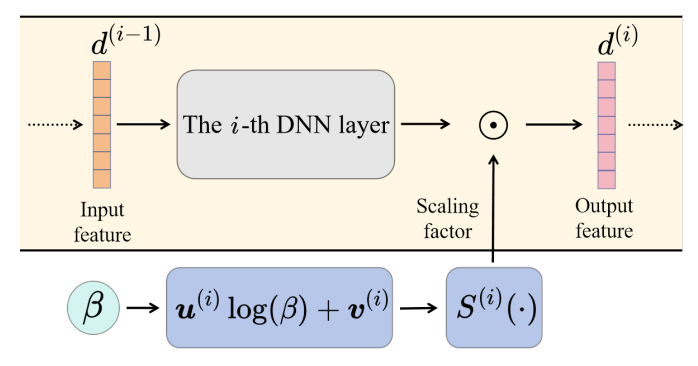


Fig. 3: Layer-wise architecture of the hypernetwork.

Let  $\mathbf{W}^{(i,c)} \in \mathbb{R}^{C_{i-1} \times K_i \times K_i}$  be the weight of the c-th filter and  $b^{(i,c)}$  be its bias. Like fully connected layers, now introducing the  $\beta$  adjustment module, the parameters are adjusted as

$$\mathbf{W}^{(i,c)}(\beta) = S^{(i,c)} \left( \mathbf{u}_{1}^{(i,c)} \log(\beta) + \mathbf{v}_{1}^{(i,c)} \right) \odot_{\text{kernel}} \mathbf{W}^{(i,c)},$$

$$b^{(i)}(\beta) = S^{(i,c)} \left( u_{2}^{(i,c)} \log(\beta) + v_{2}^{(i,c)} \right) \odot b^{(i,c)}.$$
(14)

Here,  $\boldsymbol{u}_1^{(i,c)}$ ,  $\boldsymbol{v}_1^{(i,c)} \in \mathbb{R}^{C_{i-1}}$ , and  $\boldsymbol{u}_2^{(i,c)}$ ,  $\boldsymbol{v}_2^{(i,c)} \in \mathbb{R}$ . The symbol  $\odot_{\text{kernel}}$  denotes element-wise multiplication applied to the  $K_i \times K_i$  blocks of  $\boldsymbol{W}^{(i,c)}$ . Together, the set  $\{\boldsymbol{W}^{(i,c)}, \boldsymbol{b}^{(i,c)}, \boldsymbol{u}_1^{(i,c)}, \boldsymbol{v}_1^{(i,c)}, \boldsymbol{u}_2^{(i,c)}, \boldsymbol{v}_2^{(i,c)}\}_{c=1}^{C_i}$  forms the hypernetwork parameters at the i-th layer. Compared to the original model, our hypernetwork introduces only  $2C_i(C_{i-1}+1)$  additional parameters at this layer.

# B. Hyper-VIB objective and training algorithm design

To learn the optimal hypernetworks parameters  $\phi_H$  and  $\psi_H$ , our Hyper-VIB approach adopts the following objective function:

$$C_{\text{Hyper-VIB}}(\phi_H, \psi_H) = \mathbb{E}_{\beta \sim U[a,b]} C_{\text{VIB}}(\phi_H(\beta), \psi_H(\beta)), \quad (15)$$

where the hyperparameter  $\beta$  follows the uniform distribution between [a,b]. Our optimization problem can be formulated as

$$\phi_H^*, \psi_H^* = \arg\min_{\phi_H, \psi_H} C_{\text{Hyper-VIB}}(\phi_H, \psi_H).$$
 (16)

This objective guides the hypernetworks to learn the optimal response parameters  $\phi_H(\beta)$  and  $\psi_H(\beta)$  for each fixed  $\beta$  within the range [a,b], with the goal of minimizing  $\mathcal{C}_{\text{VIB}}$ .

Using Monte Carlo sampling, we can obtain an unbiased estimation of the gradient for  $\mathcal{C}_{\text{Hyper-VIB}}$ . Specifically, during training, the hyperparameter  $\beta$  is sampled T times, and for each sampled  $\beta^{(t)}$ , given a mini-batch of data  $\{\boldsymbol{x}^{(t,m)}\}_{m=1}^{M}$ , the empirical estimation is acquired:

$$C_{\text{Hyper-VIB}} \simeq \frac{1}{T} \sum_{t=1}^{T} \frac{1}{M} \sum_{m=1}^{M} \left\{ -\log p_{\psi_{H}(\beta^{(t)})}(\boldsymbol{y}^{(t,m)} | \hat{\boldsymbol{z}}^{(t,m)}) + \beta^{(t)} D_{\text{KL}} \left( p_{\phi_{H}(\beta^{(t)})}(\hat{\boldsymbol{z}}^{(t,m)} | \boldsymbol{x}^{(t,m)}) \middle\| r(\hat{\boldsymbol{z}}^{(t,m)}) \right) \right\}.$$
(17)

Then, we propose an algorithm to learn the optimal hypernetwork parameters, as summarized in Algorithm 1.

# C. Optimality Analysis in the Linear Case

To validate the design of our hypernetwork architecture, we analyze the optimal response function under linear model

# Algorithm 1 Training Procedure for Hyper-VIB

**Input:** Training dataset  $\mathcal{D}$ , channel noise variance  $\sigma^2$ , range [a, b] for  $\beta$ .

**Output:** Optimized hypernetwork parameters  $\phi_H$ ,  $\psi_H$ .

```
1: while not converged do
 2:
         for t = 1 to T do
 3:
               Sample \beta^{(t)} \sim U[a, b]
               Select a mini-batch of data \{(\boldsymbol{x}^{(t,m)}, y^{(t,m)})\}_{m=1}^{M}
 4:
               for m = 1 to M do
 5:
                    Compute feature vector z^{(t,m)} using (1)
 6:
                    Sample noise \{\boldsymbol{\varepsilon}^{(l,m)}\}_{l=1}^L \sim \mathcal{N}(\boldsymbol{0}, \sigma^2 \boldsymbol{I})
 7:
                    Compute received vector \hat{z}^{(m)} = z^{(m)} + \varepsilon^{(l,m)}
 8:
          Compute KL-divergence using (9)
 9:
10:
          Compute loss C_{Hyper-VIB} using (17)
11:
          Update parameters via backpropagation
```

assumptions, which have been widely adopted in prior studies such as [13], [14]. Specifically, we consider the input data  $x \in \mathbb{R}^n$  and the target output  $y \in \mathbb{R}$ . On the device side, we consider a linear network  $A \in \mathbb{R}^{d \times n}$ , which uses deterministic reparameterization. On the network side, we consider a linear network  $B \in \mathbb{R}^{d \times 1}$ . The data transmission flow is

$$z = Ax, \ \hat{z} = z + \varepsilon, \ \hat{y} = B^T \hat{z}.$$
 (18)

Here,  $\varepsilon \sim \mathcal{N}(0, \sigma^2 I)$ , and we choose the MSE  $d = (y - \hat{y})^2$  to measure the distortion between y and  $\hat{y}$ .

**Theorem 1.** Consider the linear model described in (18). Given the network-side hypernetwork parameters  $\psi_H(\beta)$ , there exist device-side parameters  $\phi_H(\beta)$  in our hypernetwork such that  $\phi_H(\beta) = \phi^*(\beta)$  for all  $\beta$ , where  $\phi^*(\beta)$  is the optimal response function defined in (10).

*Proof.* Let the training set be  $\mathcal{D} = \{\boldsymbol{x}^{(i)}, y^{(i)}\}_{i=1}^N$ , organized by a matrix  $\boldsymbol{X} = [\boldsymbol{x}^{(1)}, \dots, \boldsymbol{x}^{(N)}] \in \mathbb{R}^{n \times N}$  and a vector  $\boldsymbol{y} = [y^{(1)}, \dots, y^{(N)}] \in \mathbb{R}^{1 \times N}$ , with  $N \gg n$ . With MSE, (7) yields

$$C_{\text{VIB}}(\phi, \psi) = \frac{1}{N} \sum_{i=1}^{N} \left\{ \mathbb{E}_{p_{\phi}(\hat{\boldsymbol{z}}^{(i)} | \boldsymbol{x}^{(i)})} \left[ (\hat{y}^{(i)} - y^{(i)})^{2} \right] + \beta D_{\text{KL}} \left( p_{\phi}(\hat{\boldsymbol{z}}^{(i)} | \boldsymbol{x}^{(i)}) || p(\hat{\boldsymbol{z}}^{(i)}) \right) \right\},$$
(19)

For the linear model in (18), the device-side parameters  $\phi_H(\beta)$  and network-side parameters  $\psi_H(\beta)$  correspond to  $\boldsymbol{A}$  and  $\boldsymbol{B}$ , respectively. Based on this model, we have  $\hat{\boldsymbol{z}}^{(i)} = \boldsymbol{A}\boldsymbol{x}^{(i)} + \boldsymbol{\varepsilon}^{(i)}$ , implying that  $p_{\boldsymbol{\phi}}(\hat{\boldsymbol{z}}^{(i)}|\boldsymbol{x}^{(i)}) = \mathcal{N}(\boldsymbol{A}\boldsymbol{x}^{(i)}, \sigma^2\boldsymbol{I})$ . Thus,

$$\mathbb{E}_{p_{\phi}(\hat{\boldsymbol{z}}^{(i)}|\boldsymbol{x}^{(i)})}(\hat{y}^{(i)} - y^{(i)})^{2} = \mathbb{E}[\boldsymbol{B}^{T}(\boldsymbol{A}\boldsymbol{x}^{(i)} + \boldsymbol{\varepsilon}^{(i)}) - y^{(i)}]^{2}$$

$$= (\boldsymbol{B}^{T}\boldsymbol{A}\boldsymbol{x}_{i} - y_{i})^{2} + \sigma^{2}\boldsymbol{B}^{T}\boldsymbol{B}.$$
(20)

From (9), we have

$$D_{KL}(p_{\phi}(\hat{\boldsymbol{z}}^{(i)}|\boldsymbol{x}^{(i)})||p(\hat{\boldsymbol{z}}^{(i)})$$

$$= \frac{1}{2} \left\{ (\boldsymbol{A}\boldsymbol{x}_i)^T (\boldsymbol{A}\boldsymbol{x}_i) + d(\sigma^2 - \log \sigma^2 - 1) \right\}.$$
(21)

Combining (20) and (21),  $C_{VIB}(A, B)$  can be derived as

$$C_{\text{VIB}}(\boldsymbol{A}, \boldsymbol{B}) = \frac{1}{N} \left\{ ||\boldsymbol{y} - \boldsymbol{B}^T \boldsymbol{A} \boldsymbol{X}||^2 + \frac{\beta}{2} \text{tr}(\boldsymbol{X}^T \boldsymbol{A}^T \boldsymbol{A} \boldsymbol{X}) \right\} + \sigma^2 \boldsymbol{B}^T \boldsymbol{B} + \frac{\beta}{2} \left( \sigma^2 d - d \log \sigma^2 - d \right).$$
(22)

It is evident that  $C_{VIB}(A, B)$  in (22) is a convex function with respect to A. The gradient with respect to A is

$$\frac{\partial \mathcal{C}_{\text{VIB}}(\boldsymbol{A}, \boldsymbol{B})}{\partial \boldsymbol{A}} = \frac{1}{N} \left\{ -2\boldsymbol{B}\boldsymbol{y}\boldsymbol{X}^T + 2\boldsymbol{B}\boldsymbol{B}^T\boldsymbol{A}\boldsymbol{X}\boldsymbol{X}^T + \beta\boldsymbol{A}\boldsymbol{X}\boldsymbol{X}^T \right\}. \tag{23}$$

Since  $X \in \mathbb{R}^{n \times N}$  and  $N \gg n$ ,  $XX^T$  is invertible by assuming  $\operatorname{Rank}(X) = n$ . Setting the gradient in (23) to zero yields

$$\mathbf{A}^* = \left(\mathbf{B}\mathbf{B}^T + \frac{1}{2}\beta\mathbf{I}\right)^{-1}\mathbf{B}\mathbf{y}\mathbf{X}^T(\mathbf{X}\mathbf{X}^T)^{-1}, \qquad (24)$$

which is the closed-form solution for the optimal response function on the device side with fixed B. Clearly,  $A^*$  depends on  $\beta$  and varies with  $\beta$ .

We now prove that there exist parameters in our hypernetwork that can represent  $A^*$ . Consider the singular value decomposition of  $B = U\Sigma V^T$ , where  $U \in \mathbb{R}^{d\times d}$  is a unitary orthogonal matrix,  $\Sigma \in \mathbb{R}^{d\times 1}$  is a vector with only the first element equal to ||B||, and the rest are zeros, while V is essentially a scalar 1. Then  $A^*$  can be expressed as

$$\boldsymbol{A}^* = \boldsymbol{U} \left( \boldsymbol{\Sigma} \boldsymbol{\Sigma}^T + \frac{1}{2} \beta \boldsymbol{I} \right)^{-1} \boldsymbol{\Sigma} \boldsymbol{y} \boldsymbol{X}^T (\boldsymbol{X} \boldsymbol{X}^T)^{-1}.$$
 (25)

Consider the device-side network as a two-layer structure with  $\boldsymbol{W}^{(2)}=2\boldsymbol{U}$  and  $\boldsymbol{W}^{(1)}=\frac{1}{||\boldsymbol{B}||^2}\boldsymbol{\Sigma}\boldsymbol{y}\boldsymbol{X}^T(\boldsymbol{X}\boldsymbol{X}^T)^{-1}$ . For the first-layer  $\beta$  adjustment module, let  $\boldsymbol{u}^{(1)}=-1\cdot \mathbf{1}$  and  $\boldsymbol{v}^{(1)}=(\ln 2+2\ln ||\boldsymbol{B}||)\cdot \mathbf{1}$ , where  $\mathbf{1}\in\mathbb{R}^d$  is the all-ones vector. Therefore, we have

$$S^{(1)}(\boldsymbol{u}^{(1)}\log(\beta)+\boldsymbol{v}^{(1)}) = \frac{1}{1+\frac{1}{2}||\boldsymbol{B}||^{-2}\beta} \cdot 1 = \frac{||\boldsymbol{B}||^2}{||\boldsymbol{B}||^2+\frac{1}{2}\beta} \cdot 1. (26)$$

Continuing the derivation, we get

$$\boldsymbol{W}^{(1)}(\beta) = S^{(1)}(\boldsymbol{u}^{(1)}\log(\beta) + \boldsymbol{v}^{(1)}) \odot_{\text{row}} \boldsymbol{W}^{(1)}$$

$$= \operatorname{diag}\left(\frac{||\boldsymbol{B}||^2}{||\boldsymbol{B}||^2 + \frac{1}{2}\beta}\right) \cdot \frac{1}{||\boldsymbol{B}||^2} \boldsymbol{\Sigma} \boldsymbol{y} \boldsymbol{X}^T (\boldsymbol{X} \boldsymbol{X}^T)^{-1}$$

$$= \left(\boldsymbol{\Sigma} \boldsymbol{\Sigma}^T + \frac{1}{2}\beta\right)^{-1} \boldsymbol{\Sigma} \boldsymbol{y} \boldsymbol{X}^T (\boldsymbol{X} \boldsymbol{X}^T)^{-1},$$
(27)

where  $\operatorname{diag}(x)$  represents a diagonal matrix in  $\mathbb{R}^{d \times d}$  with all diagonal elements are x. For the second layer, setting both  $\boldsymbol{u}^{(2)}$  and  $\boldsymbol{v}^{(2)}$  to zero vectors yields

$$\mathbf{W}^{(2)}(\beta) = S^{(2)}(\mathbf{u}^{(2)}\log(\beta) + \mathbf{v}^{(2)}) \odot_{\text{row}} \mathbf{W}^{(2)} = \mathbf{U}.$$
 (28)

According to (25), (27) and (28), we have

$$A^* = W^{(2)}(\beta)W^{(1)}(\beta). \tag{29}$$

Finally, by setting  $\phi_H(\beta) = \mathbf{W}^{(2)}(\beta)\mathbf{W}^{(1)}(\beta)$ , we conclude that for any  $\beta$ , when  $\psi_H(\beta) = \mathbf{B}$  is given,  $\phi_H(\beta)$  is the optimal response function for  $\beta$ .

## IV. NUMERICAL RESULTS AND DISCUSSIONS

This section evaluates the performance of the proposed Hyper-VIB approach in device-network collaborative intelligence, highlighting its efficiency in enabling task-oriented communications.

# A. Experimental Settings

We consider classification and regression tasks. For classification, we use the MNIST [21] and CIFAR-10 [22] datasets.

Tasks	Dataset	Methods	Parameters	Time(s)
Classification	MNIST	VIB	$18.81 \times 10^{4}$	3,103
		Hyper-VIB	$18.94 \times 10^{4}$	696
	CIFAR-10	VIB	$40.46 \times 10^{5}$	236,800
		Hyper-VIB	$41.81 \times 10^{5}$	31,640
Regression	Bluetooth	VIB	$55.92 \times 10^{4}$	1,759
		Hyper-VIB	$56.21 \times 10^{4}$	479
	WIFI	VIB	$65.42 \times 10^4$	2,042
		Hyper-VIB	$66.48 \times 10^4$	584

TABLE I: Comparison of parameter counts and training time between VIB and proposed Hyper-VIB.

For regression, we study wireless localization in multipath environments using simulated Bluetooth and WiFi ranging data. The simulated datasets for received signals are generated based on the Bluetooth two-way channel model [23] and the WiFi channel model [24], with the target output being the estimated line-of-sight (LoS) propagation time between transceivers. To assess the impact of the hypernetwork, we compare Hyper-VIB with the classical VIB method [3], [25]. For a fair comparison, both Hyper-VIB and VIB use identical DNN architectures, including fully connected layers and convolutional neural networks. For Hyper-VIB, a single training run is conducted with  $\beta$  values ranging from  $10^{-5}$  to 1. For VIB, a grid search is performed, where training is conducted separately for each  $\beta$  to determine the optimal value. We use top-1 accuracy for classification performance and mean squared error (MSE) of propagation time for localization accuracy. The signal-to-noise ratio (SNR) is set to 20 dB, and the feature dimension z is fixed at 64.

# B. Experimental Results

In our experiments, to determine the hyperparameter  $\beta$ , Hyper-VIB is trained once over the range  $[10^{-5}, 1]$ . After training, we sample  $\beta$  every 0.5 orders of magnitude and use the hypernetwork to directly generate the corresponding model parameters for evaluation, selecting the  $\beta$  that achieves the best performance. In contrast, VIB performs a grid search over the same  $\beta$  range, training a separate model for each sampled value, and selects the  $\beta$  that yields the best performance.

Firstly, we compare the training time and parameter count of Hyper-VIB and VIB across multiple datasets. As shown in Table I, Hyper-VIB achieves a substantial improvement in training efficiency, reducing training time by approximately 80% compared to VIB. This efficiency gain is attributed to the introduction of a hypernetwork, which allows Hyper-VIB to be trained only once and eliminates the need for retraining across all  $\beta$  values, as required by VIB's grid search. In terms of parameter count, Hyper-VIB is nearly identical to VIB, as only the  $\beta$  adjustment module in the hypernetwork adds a negligible number of additional parameters.

Then, we compare the performance of Hyper-VIB and VIB. As shown in Fig. 4, across all four datasets, Hyper-VIB consistently outperforms or rivals VIB for all  $\beta$  values, and when both methods achieve peak performance respectively, the corresponding trade-off hyperparameter  $\beta$  exhibits closely aligned values. This demonstrates the effectiveness of

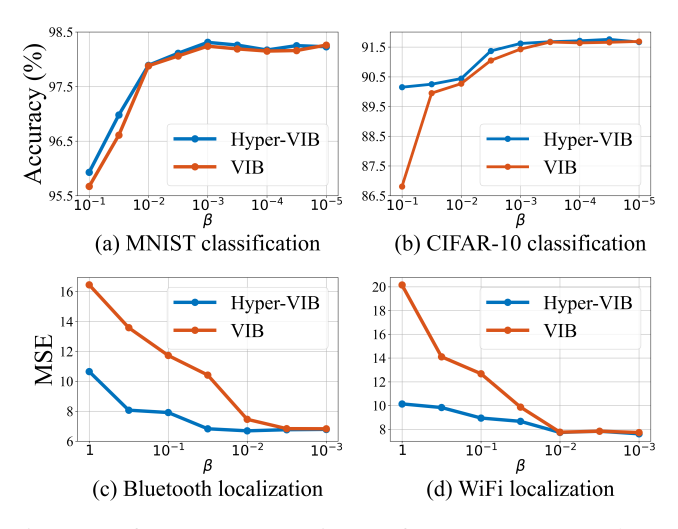


Fig. 4: Performance comparisons of our Hyper-VIB scheme with the conventional VIB benchmark, under varying  $\beta$  values for different tasks.

the hypernetwork in Hyper-VIB at approximating the bestresponse function from  $\beta$  to model parameters. As a result, Hyper-VIB requires only a single training run to generate model parameters for all  $\beta$  values, evaluate their performance, and efficiently identify the optimal one, thereby significantly reducing training time and computational cost.

It can be observed from Fig. 4 that a smaller  $\beta$  improves the accuracy in classification tasks, and reduces the regression errors in localization tasks. In addition, if  $\beta$  is large and far from the optimal region, VIB shows a fast drop in performance. This is because VIB trains separate models for each fixed  $\beta$ , making it highly sensitive to hyperparameter values. Instead, Hyper-VIB undergoes a single training run over all values of  $\beta$  and shares most model weights through the hypernetwork. As such, it can maintain a relatively better performance with a suboptimal  $\beta$ . Therefore, within a wide range of  $\beta$  values, Hyper-VIB demonstrates a significant performance gain over VIB, highlighting its superior robustness.

## V. CONCLUSION

In this paper, we proposed Hyper-VIB, a novel hypernetwork-enhanced information bottleneck framework for efficient task-oriented communications in 6G collaborative intelligent systems. Our approach leverages IB theory to jointly train the device-side and network-side models, which can achieve the minimal communication overhead and maximal task accuracy simultaneously. Hyper-VIB employs hypernetworks to optimize the trade-off hyperparameter  $\beta$ , which balances task accuracy against communication costs. Specifically, the hypernetwork generates approximately optimal DNN parameters for all  $\beta$  values within a single training phase, enabling efficient hyperparameter selection. We further provide theoretical validation through linear case analysis of the hypernetwork design. Experiments verify that Hyper-VIB achieves higher accuracy and training efficiency than classical VIB in both classification and regression tasks.

### REFERENCES

- [1] ITU Radiocommunication Sector, "Framework and overall objectives of the future development of IMT for 2030 and beyond," International Telecommunication Union Radiocommunication Sector (ITU-R), Technical Report, Tech. Rep., 2023.
- [2] H. Yang and M. S. Alouini, "Data-oriented transmission in future wireless systems: Toward trustworthy support of advanced internet of things," *IEEE Veh. Technol. Mag.*, vol. 14, no. 3, pp. 78–83, Sep. 2019.
- [3] J. Shao, Y. Mao, and J. Zhang, "Learning task-oriented communication for edge inference: An information bottleneck approach," *IEEE J. Sel. Areas Commun.*, vol. 40, no. 1, pp. 197–211, Jan. 2022.
- [4] Y. Shi, Y. Zhou, D. Wen, Y. Wu, C. Jiang, and K. B. Letaief, "Task-oriented communications for 6G: Vision, principles, and technologies," *IEEE Wireless Commun.*, vol. 30, no. 3, pp. 78–85, Jun. 2023.
- [5] S. Xie, S. Ma, M. Ding, Y. Shi, M. Tang, and Y. Wu, "Robust information bottleneck for task-oriented communication with digital modulation," *IEEE J. Sel. Areas Commun.*, vol. 41, no. 8, pp. 2577– 2591, Aug. 2023.
- [6] N. Tishby, F. C. Pereira, and W. Bialek, "The information bottleneck method," arXiv preprint physics/0004057, 2000.
- [7] M. Moldoveanu and A. Zaidi, "On in-network learning. a comparative study with federated and split learning," in *Proc. IEEE SPAWC*, Sep. 2021, pp. 221–225.
- [8] M. Moldoveanu and A. Zaidi, "In-network learning: Distributed training and inference in networks," *Entropy*, vol. 25, no. 6, p. 920, Jun. 2023.
- [9] J. Shao, Y. Mao, and J. Zhang, "Task-oriented communication for multidevice cooperative edge inference," *IEEE Trans. Wireless Commun.*, vol. 22, no. 1, pp. 73–87, Jan. 2023.
- [10] J. Peng, B. Ren, L. Yang, C. Peng, P. Niu, and H. Wu, "QML-IB: Quantized collaborative intelligence between multiple devices and the mobile network," in *Proc. IEEE ISIT*, Jul. 2024, pp. 2454–2459.
- [11] J. Snoek, O. Rippel, K. Swersky, R. Kiros, N. Satish, N. Sundaram, M. Patwary, M. Prabhat, and R. Adams, "Scalable Bayesian optimization using deep neural networks," in *Proc. ICML*. PMLR, Jul. 2015, pp. 2171–2180.
- [12] D. Ha, A. Dai, and Q. V. Le, "Hypernetworks," arXiv preprint arXiv:1609.09106, 2016.
- [13] J. Bae, M. R. Zhang, M. Ruan, E. Wang, S. Hasegawa, J. Ba, and R. B. Grosse, "Multi-rate VAE: Train once, get the full rate-distortion curve," in *Proc. ICLR*, 2023.
- [14] M. Mackay, P. Vicol, J. Lorraine, D. Duvenaud, and R. Grosse, "Self-tuning networks: Bilevel optimization of hyperparameters using structured best-response functions," in *Proc. ICLR*, 2019.
- [15] R. Gibbons et al., "A primer in game theory," 1992.
- [16] S. Xie, H. He, H. Li, S. Song, J. Zhang, Y. J. A. Zhang, and K. B. Letaief, "Deep learning-based adaptive joint source-channel coding using hypernetworks," in *Proc. IEEE MeditCom*, Jul. 2024, pp. 191–196
- [17] D. P. Kingma, T. Salimans, and M. Welling, "Variational dropout and the local reparameterization trick," *Proc. NeuIPS*, vol. 28, 2015.
- [18] T. M. Cover, Elements of information theory. John Wiley & Sons, 1999.
- [19] D. P. Kingma and M. Welling, "Auto-encoding variational Bayes," arXiv preprint arXiv:1312.6114, 2013.
- [20] A. A. Alemi, I. Fischer, J. V. Dillon, and K. Murphy, "Deep variational information bottleneck," in *Proc. ICLR*, 2016.
- [21] Y. LeCun, L. Bottou, Y. Bengio, and P. Haffner, "Gradient-based learning applied to document recognition," *Proc. IEEE*, vol. 86, no. 11, pp. 2278–2324, Nov. 1998.
- [22] A. Krizhevsky, G. Hinton et al., "Learning multiple layers of features from tiny images," University of Toronto, Toronto, ON, Canada, Tech. Rep., 2009.
- [23] Z. B. Tariq, J. P. Van Marter, A. G. Dabak, N. Al-Dhahir, and M. Torlak, "Reduced complexity deep learning approach for Bluetooth ranging in multi-path environments," *IEEE Sens. J.*, vol. 24, no. 19, pp. 31431– 31441, Oct. 2024.
- [24] M. Kotaru, K. Joshi, D. Bharadia, and S. Katti, "SpotFi: Decimeter level localization using WIFI," SIGCOMM Comput. Commun. Rev., vol. 45, no. 4, p. 269–282, Aug. 2015.
- [25] W. Qian and F. Gechter, "Variational information bottleneck model for accurate indoor position recognition," in *Proc. IEEE ICPR*, Jan. 2021, pp. 2529–2535.